


RESEARCH ARTICLE

Open Access



Famotidine activates the vagus nerve inflammatory reflex to attenuate cytokine storm

Huan Yang^{1*†} , Sam J. George^{1†}, Dane A. Thompson^{1,2}, Harold A. Silverman¹, Téa Tsaava¹, Aisling Tynan¹, Valentin A. Pavlov^{1,2,3}, Eric H. Chang^{1,2,3}, Ulf Andersson⁴, Michael Brines¹, Sangeeta S. Chavan^{1,2,3*} and Kevin J. Tracey^{1,2,3*}

Abstract

Background: Severe COVID-19 is characterized by pro-inflammatory cytokine release syndrome (cytokine storm) which causes high morbidity and mortality. Recent observational and clinical studies suggest famotidine, a histamine 2 receptor (H2R) antagonist widely used to treat gastroesophageal reflux disease, attenuates the clinical course of COVID-19. Because evidence is lacking for a direct antiviral activity of famotidine, a proposed mechanism of action is blocking the effects of histamine released by mast cells. Here we hypothesized that famotidine activates the inflammatory reflex, a brain-integrated vagus nerve mechanism which inhibits inflammation via alpha 7 nicotinic acetylcholine receptor ($\alpha 7nAChR$) signal transduction, to prevent cytokine storm.

Methods: The potential anti-inflammatory effects of famotidine and other H2R antagonists were assessed in mice exposed to lipopolysaccharide (LPS)-induced cytokine storm. As the inflammatory reflex is integrated and can be stimulated in the brain, and H2R antagonists penetrate the blood brain barrier poorly, famotidine was administered by intracerebroventricular (ICV) or intraperitoneal (IP) routes.

Results: Famotidine administered IP significantly reduced serum and splenic LPS-stimulated tumor necrosis factor (TNF) and IL-6 concentrations, significantly improving survival. The effects of ICV famotidine were significantly more potent as compared to the peripheral route. Mice lacking mast cells by genetic deletion also responded to famotidine, indicating the anti-inflammatory effects are not mast cell-dependent. Either bilateral sub-diaphragmatic vagotomy or genetic knock-out of $\alpha 7nAChR$ abolished the anti-inflammatory effects of famotidine, indicating the inflammatory reflex as famotidine's mechanism of action. While the structurally similar H2R antagonist tiotidine displayed equivalent anti-inflammatory activity, the H2R antagonists cimetidine or ranitidine were ineffective even at very high dosages.

Conclusions: These observations reveal a previously unidentified vagus nerve-dependent anti-inflammatory effect of famotidine in the setting of cytokine storm which is not replicated by high dosages of other H2R antagonists in clinical use. Because famotidine is more potent when administered intrathecally, these findings are also consistent with a primarily central nervous system mechanism of action.

Keywords: Histamine, Histamine receptors, Vagus nerve signaling, Cholinergic anti-inflammatory pathway

[†]Huan Yang and Sam J. George contributed equally to this work

*Correspondence: hyang@northwell.edu; schavan@northwell.edu; kjtracey@northwell.edu

¹Institute for Bioelectronic Medicine, The Feinstein Institutes for Medical Research, 350 Community Drive, Manhasset, NY 11030, USA
Full list of author information is available at the end of the article

Introduction

The recent emergence and rapid spread of the SARS-CoV-2 virus has resulted in a catastrophic COVID-19 pandemic characterized by high morbidity and mortality. Emerging evidence suggests that dysregulated immune



responses play a critical role in fueling a cascade of excessive inflammation which is a key feature of severe COVID-19 (Mehta et al. 2020; Wang et al. 2020; Jafarzadeh et al. 2020; Moore and June 2020). The hyperactive inflammatory response elicited by severe acute respiratory syndrome coronavirus 2 (SARS-CoV-2) frequently culminates in the cytokine release syndrome (cytokine storm). Critical features of cytokine storm involve the infiltration, expansion and activation of monocytes and macrophages and other immune competent cells with the consequent excessive production of pro-inflammatory cytokines and chemokines, e.g., TNF and IL-6 (Mehta et al. 2020; Moore and June 2020), which drive the clinical course, e.g., causing acute respiratory distress syndrome (Jafarzadeh et al. 2020).

Many drugs have been evaluated as potential treatments of the inflammatory components of COVID-19, but few compounds have improved outcome. Among these, anti-IL-6 biologicals and high dose glucocorticoids may benefit patients undergoing cytokine storm (Moore and June 2020; Sharun et al. 2020). However, anti-IL-6 therapy targets only a single component of a complicated pro-inflammatory cascade and incompletely blocks inflammatory processes. Although glucocorticoids more broadly suppress the inflammatory response, their use is associated with impaired clearance of viral load, as well as associated serious potential adverse effects in many tissues (Theoharides and Conti 2020). Therefore, a search for additional pharmacological approaches to inhibit lethal cytokine storm is warranted.

Several observational studies of COVID-19 patients indicate famotidine, a selective H2R antagonist widely used to treat gastroesophageal reflux disease, improves survival in hospitalized patients and ameliorates symptoms in non-hospitalized patients (Janowitz et al. 2020; Freedberg et al. 2020) when administered at a high dose. A recent randomized placebo-controlled and double-blinded clinical trial has shown that high dose oral famotidine administered to symptomatic, non-hospitalized COVID-19 patients accelerates the suppression of interferon γ and improves symptom resolution (Brennan et al. 2022). Although these and other clinical findings are potentially important, enthusiasm for using famotidine has been hampered because the molecular mechanism of action underlying famotidine's beneficial effects remains enigmatic.

The chemical structure of famotidine led some to theorize it might interfere with the viral proteases required for SARS-CoV-2 replication, but *in silico* studies indicate famotidine does not inhibit either SARS-CoV-2 proteases or SARS-CoV-2 viral replication

(Loffredo, et al. 2020; Wu et al. 2020; Malone, et al. 2020). Pharmacologically, famotidine is classified as an inverse agonist, i.e., a competitive antagonist of histamine-induced receptor activation, while also decreasing baseline H2R signaling (Panula et al. 2015). Famotidine has been implicated as an inhibitor of histamine-induced toll-like receptor 3-mediated inflammatory signaling in SARS-CoV-2 infected cells *in vitro* (Mukherjee et al. 2021). Famotidine may also act through other on-target histaminergic mechanisms via gastric acid reduction (Malone, et al. 2020; Aguila and Cua 2020) or immune cell generation of pro-inflammatory mediators (Malone, et al. 2020; Lam et al. 2021; Ennis and Tiligada 2020). Additionally, potentially relevant off-target effects of famotidine include scavenging reactive oxygen radicals, especially the hydroxyl ion (Ahmadi et al. 2011; Ching et al. 1994, 1993; Lapenna et al. 1994; Zyl et al. 1993), which may reduce secondary inflammation and damage. Accordingly, the mechanistic basis for the beneficial effects of famotidine in COVID remain unidentified. Because H2 antagonists are polar, and do not readily pass the blood brain barrier, we reasoned here that the high dose requirements for famotidine efficacy might be attributable to targeting in the central nervous system (CNS), which abundantly expresses all four histamine receptors (Panula et al. 2015; Haas et al. 2008).

The inflammatory reflex is a vagus nerve mediated homeostatic mechanism which inhibits cytokine storm. Vagus nerve signals arising in the brain stem attenuate inflammation by cholinergic signal transduction which activates the $\alpha 7$ nicotinic acetylcholine receptor ($\alpha 7$ nAChR) expressed on cytokine producing cells and thereby inhibiting cytokine release (Gauthier et al. 2021). Since H2R is expressed in the central nervous system, we used a murine model of cytokine storm to assess the role of famotidine in stimulating the inflammatory reflex (Ramos-Benitez et al. 2018; Smuda et al. 2011). The results indicate that famotidine inhibits endotoxin-induced cytokine storm and improves survival via a vagus nerve dependent, but histamine H2 receptor-independent mechanism.

Materials and methods

Lipopolysaccharide (*E. coli*. 0111:B4, Cat# L2630), histamine (Cat # H7125), ranitidine (Cat # R101), famotidine (Cat # F6889) and cimetidine (Cat # C4522) were purchased from Sigma (St. Louis, MO). Famotidine (iv vial, 20 mg/2 ml) was from APP Pharmaceutical LLC (Schaumburg, IL). Tiotidine (Cat # 0826) was from Tocris Bioscience (Minneapolis, MN). Fetal bovine serum was

obtained from Gibco BRL (Carlsbad, CA). Glutamine was from Biowhittaker Inc., (Walkersville, MD). Thioglycollate medium was purchased from Becton Dickinson Co., (Sparks, MD). Protease inhibitor minitabets (Cat # A32953) were from Thermo Fisher Scientific Inc., (Waltham, MA).

Cell culture

Murine macrophage-like RAW 264.7 cells were obtained from American Type Culture Collection (Rockville, MD). RAW 264.7 cells were cultured in DMEM or in RPMI 1640 medium, respectively, supplemented with 10% fetal bovine serum, 100 U/ml penicillin and 100 µg/ml streptomycin. Thioglycollate-elicited peritoneal macrophages were maintained in RPMI 1640 medium before use. Cells in culture plates were used at 90% confluence. Stimulation to cells was carried out in serum-free Opti-MEM I medium (Life Technologies, Carlsbad, CA).

Primary mouse thioglycollate-elicited macrophages were obtained as previously described (Yang et al. 2015). Briefly, each mouse was injected intraperitoneally with 2 ml of thioglycollate broth (4%). Two days later, mice were euthanized and 5 ml of 11.6% sterile sucrose was injected into the peritoneal cavity. Lavage fluid from peritoneal cavity (containing macrophages) was collected by using BD insyte autoguard (BD bioscience, San Jose, CA). Cells were then passed through a strainer (BD Falcon, Franklin Lakes, NJ) to remove debris. After washing with RPMI medium, cells were suspended in RPMI 1640 medium supplemented with 10% heat-inactivated fetal bovine serum (FBS), 2 mM glutamine and 100 U/mL penicillin, 100 µg/mL streptomycin. Cells were seeded in 96-well Primaria tissue culture dishes (Life Technologies, Grand Island, NY) and allowed to rest for 18–24 h at 37 °C incubator. All treatments were carried out in serum free Opti-MEM I medium (Life Technologies).

Animal experiments

Animals

Male C57BL/6, $\alpha 7$ nicotinic acetylcholine receptor knockout (stock # B6.129S7-Chrna7^{<tm1Bay>/J}) mice or mast cell deficient *Kit*^{W^{-sh}}/*Kit*^{W^{-sh}} sash mice (stock # 030,764, C57BL/6 J-congenic *Kit*^{W^{-sh}}) (all 8–12 weeks old), were obtained from the Jackson Laboratories (Bar Harbor, ME) and acclimated for at least 1 week before conducting experiments. All animal procedures were approved by the Feinstein Institutes for Medical Research Institutional Animal Care and Use Committee (IACUC, protocol #2016–028). Mice were housed in the Center for Comparative Physiology of the Feinstein Institutes for Medical Research under standard temperature, light and dark cycle conditions.

Vagotomy and transgastric pyloric dilation surgery

Surgery for bilateral sub-diaphragmatic vagotomy was performed following the published methods (Dezfuli et al. 2018). Mice were anesthetized with isoflurane (2%) and oxygen (1.25 l/min) and placed in a supine position and a midline celiotomy was made. Visceral organs were moved to the right, exposing the esophagus. Left and right vagus nerves were identified and transected just inferior to the diaphragm. The abdomen was then closed with sutures and/or staples.

Transgastric pyloric dilation surgery. This procedure was performed following bilateral sub-diaphragmatic vagotomy surgery in order to reduce the side effects of stomach distension following vagotomy, as vagus nerve controls stomach emptying. Following induction of anesthesia with intramuscular injection of a mixture of ketamine (50 mg/kg) and xylazine (10 mg/kg), the mouse was fixed in supine position. A midline celiotomy was made and carried superiorly to the xyphoid process in order to ensure the best visualization of the foregut structures. A small retractor (2.75" Alm Retractor, Cat# RS6510, Roboz Surgical Instrument Co., Gaithersburg, MD) was placed in the celiotomy to provide exposure. The anterior surface of the stomach was brought into the field of view with gentle, caudal retraction of the transverse colon. A space on the greater curvature of the stomach, without obvious surface vessels or mesocolic attachment, approximately 2 cm from the pylorus was identified and stabilized with a forceps. A 0.5 cm gastrotomy was made and the pylorus was accessed through the stomach for serial dilation, beginning with a 2 mm probe and concluding with a 4 mm probe (coated in water-soluble lubricant, Surgilube, HR Pharmaceuticals, York, PA), progressing in 0.5 mm increments (Cat #S1599-7002, Garrett Vascular Dilator precision medical device Inc., Hawthorne, NY). Once the probe is through the muscle, the probe was left in place for one minute to ensure adequate dilation. Following dilation, a 5–0 Vicryl suture was used to close the gastrotomy. Following surgery, warm saline (1 ml) was administered subcutaneously, and mice were placed in a warm cage to recover. Liquid diet was provided for 3–5 days post-surgery.

Intracerebroventricular (ICV) Injection

The procedure was performed following published method (DeVos and Miller 2013). Mice were anesthetized with a mixture of ketamine (50 mg/kg) and xylazine (10 mg/kg) and placed in a stereotactic head frame using ear bars (Stoelting Co. Wood Dale, IL). The incisor bar was adjusted until the plane defined by the lambda, and

bregma was parallel to the base plate. A midline skin incision on the brain was made and the fascia is separated. The needle of a Hamilton syringe (10 μ l) was stereotactically guided into the right lateral ventricle (1.2 mm lateral to the right, 0.6 mm posterior, 2.1 mm depth/ventral) at a rate of 1 mm/min. Once the needle of the Hamilton syringe was inserted, test compound or vehicle (in 5 μ l volume) was injected into the right lateral ventricle (1 μ l/min) and withdrawal of the syringe was performed slowly (4–5 min) to prevent backflow. The incision was sutured shut with 5–0 vicryl suture and 1 ml of saline was injected subcutaneously. Mice were allowed to recover in a clean cage near a heat lamp.

Electrophysiological recording

The vagus nerve recordings were performed as described previously (Steinberg et al. 2016; Zanos et al. 2018). Briefly, C57BL/6 mice were anesthetized using isoflurane at 2.5% in 100% oxygen at a flow rate of 1 l/min, and maintained at 1.5% isoflurane on a heating pad to keep the core body temperature around 37 °C. In prone position the animal's head was fixed in a stereotactic frame. The sterile 26G stainless steel cannula (Plastics One, Inc.) was inserted into the left lateral ventricle using the coordinates from Paxinos and Franklin atlas and secured using Vetbond (Butler Schein, Dublin, OH). The animals were then repositioned in the left lateral recumbent, and the vagus nerve was isolated from the carotid sheath. Platinum-iridium cuff electrodes (CorTec, Freiburg, Germany) were placed on the nerve with reference electrode set in the neck muscle. Electrophysiological signals were recorded using a Plexon data-acquisition system (OmniPlex, Plexon, Inc.) at 40 kHz sampling rate. Vagus nerve activity was acquired for 30 min prior to and post-ICV administration of either 5 μ l 0.4 mg/mL Famotidine or normal Saline (BD, Franklin Lakes, NJ). The electrophysiological signals were analyzed using Spike2 software (CED, Cambridge, England) as described previously (Zanos et al. 2018).

LPS toxicity in mice

C57BL/6 or α 7nAChR knockout mice (male, 8–12 weeks of age) had intraperitoneal injection of LPS (6–7 mg/kg) and treated with test compound or vehicle control administered IP or ICV either immediately after LPS injection or, in some experiments, prior to LPS injection at times indicated in the text. Two and half or 6 h later, mice were euthanized, serum and spleen were collected for analyses.

Cytokine measurements

Mouse TNF, IL-6, IL-1 β , CXCL1 in cell culture supernatants or in samples of mouse serum or spleen were

measured by commercially obtained ELISAs as per manufacturer's instructions (R & D System Inc., Minneapolis, MN). Mouse splenic tissue was added to 1XPBS (400 μ l per spleen) containing protease inhibitor and homogenized for 30 s using Polytron homogenizer PT 3100 (VWR Scientific, Radnor, PA). The homogenate was then centrifuged at 2000 rpm at 4C for 20 min. Supernatants were collected and transferred to a fresh tube. Protein concentration was measured using Bradford assay (Thermo Fisher).

Statistical analysis

All data were analyzed using Prism 8.0 (GraphPad Prism) and were presented as means \pm SEM. Differences between treatment groups were determined by student's t test for comparison of two groups. For comparison of more than 2 groups, analysis was performed using one-way ANOVA followed by Tukey's multiple comparisons test. In animal survival studies, differences between treatment groups were determined using 2-tailed Fisher's exact test. P values less than 0.05 were considered statistically significant.

Results

Famotidine attenuates LPS-induced pro-inflammatory cytokine release and improves survival.

To assess the potential role of famotidine in inflammation, we evaluated its effects on LPS-induced cytokine storm, a process driven in large part by the key pro-inflammatory cytokines TNF and IL-6 (Ramos-Benitez et al. 2018). C57BL/6 mice were administered famotidine (FM; 0.4 or 4 mg/kg, which corresponds (Nair and Jacob 2016) to a subtherapeutic versus therapeutic human equivalent dose of \sim 2 mg and \sim 20 mg respectively) or vehicle intraperitoneally 30 min prior to LPS (7 mg/kg). The animals were then euthanized at 2.5 h post-LPS exposure, a timepoint appropriate for capture of both TNF and IL-6 release (Seemann et al. 2017). Intraperitoneal administration of famotidine reduced LPS-induced TNF levels in a dose-dependent manner. The higher dose of famotidine significantly reduced LPS-induced elevated levels of serum and splenic TNF by \sim 40% and \sim 65% respectively and IL-6 by \sim 40% and \sim 50% (Fig. 1A–D). However, the suppressive effects of famotidine did not extend to IL-1 β and CXCL1 within the serum and spleen at this timepoint, or 6 h later (Additional file 1: Fig. S1), suggesting a narrow anti-inflammatory target for famotidine's early effects. Further, by 6 h following LPS administration, famotidine no longer significantly altered serum or spleen IL-6 levels as compared to vehicle (Additional file 1: Fig. S1D,G), indicating a short biological half-life

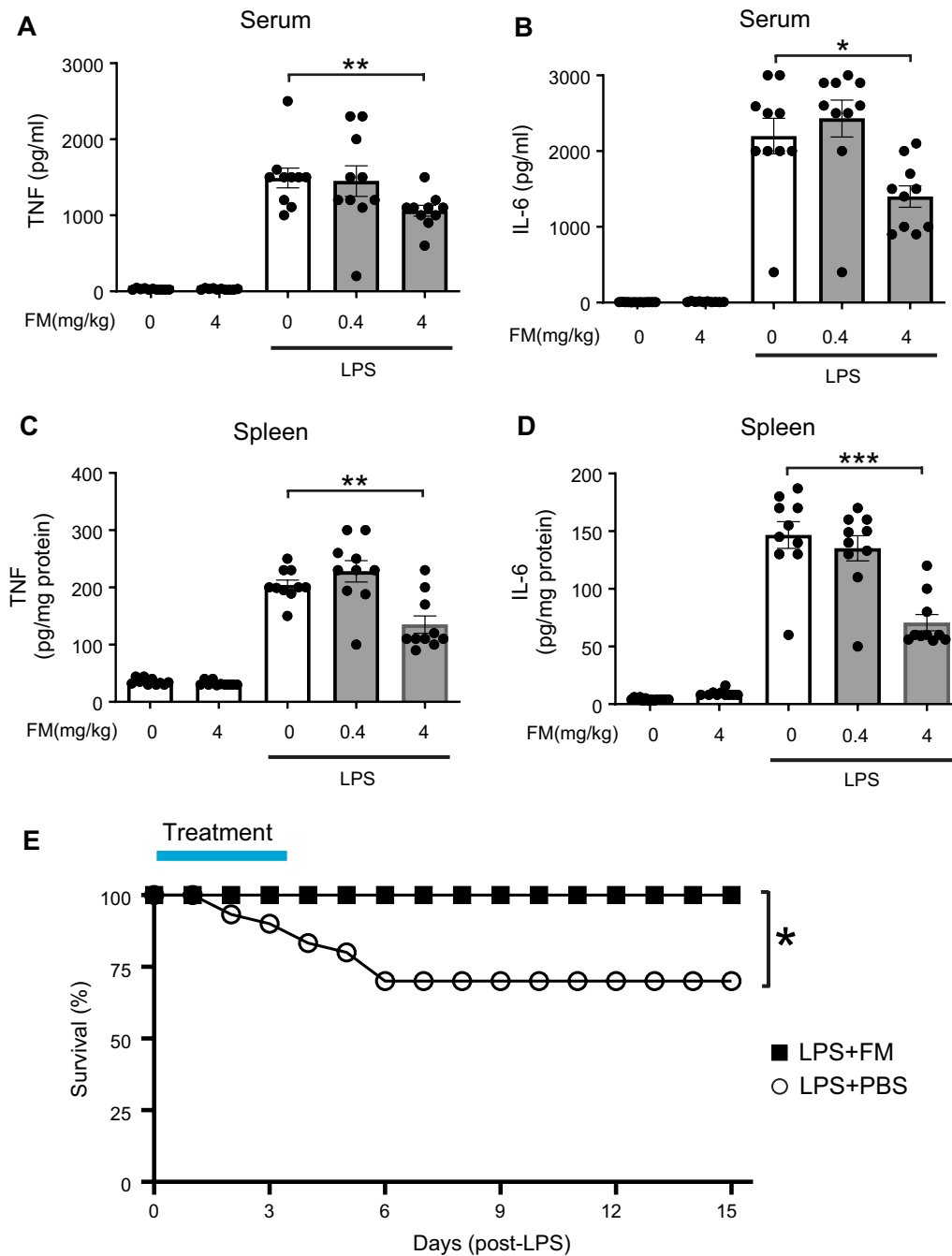


Fig. 1 Famotidine attenuates lipopolysaccharide (LPS)-induced inflammatory responses in mice. **A–D** Male C57BL/6 mice, 8–12 weeks of age, were injected with LPS (7 mg/kg) with or without famotidine (FM, 0.4 or 4 mg/kg, in 100 µl volume), intraperitoneally (IP) 30 min before LPS injection. Mice were euthanized 2.5 h after LPS administration and serum and spleen TNF and IL-6 were measured. N = 10 mice per group. *P < 0.01, **P = 0.001, ***P < 0.001. **E** Male C57BL/6 mice, 8–12 weeks old, were injected with LPS (6 mg/kg, IP). Famotidine (FM, 4 mg/kg) or PBS (in 100 µl volume) were injected intraperitoneally twice a day for 3 days, survival was monitored for 2 weeks. N = 30 mice per group. *P = 0.001 vs. LPS + PBS group

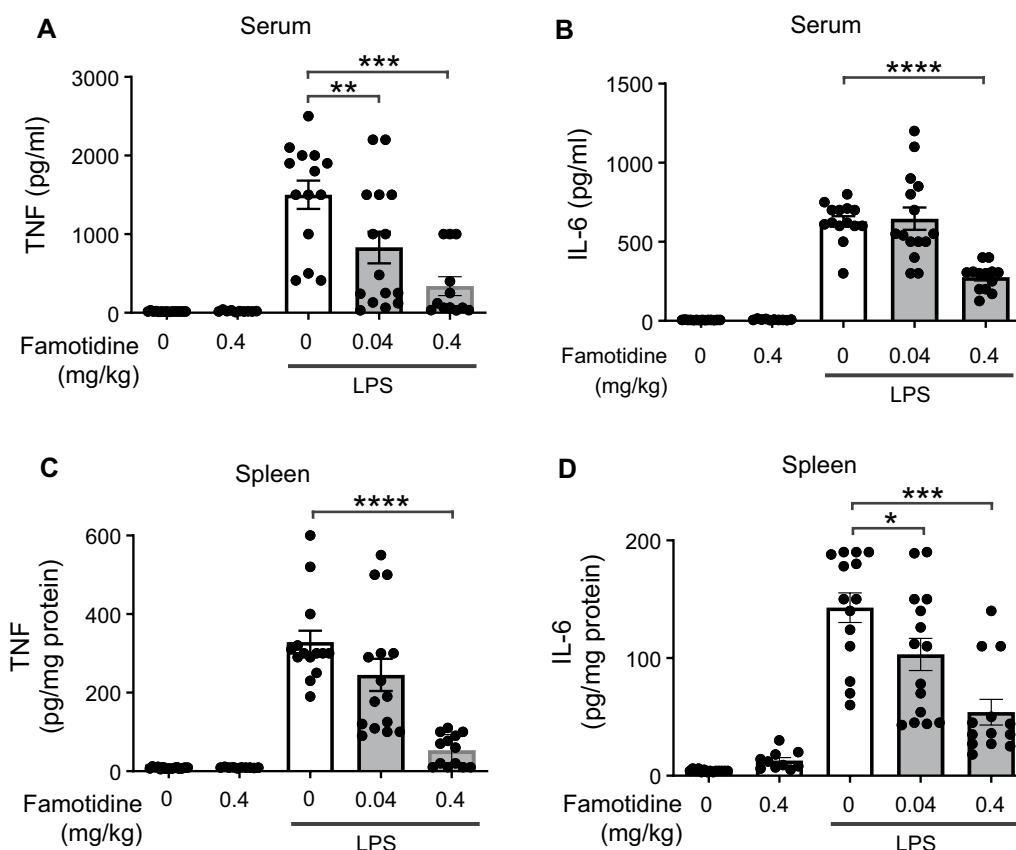


Fig. 2 Famotidine is more potent when administered into the central nervous system. **A–D** Famotidine (intracerebroventricular, ICV) injection attenuated LPS-induced systemic TNF and IL-6 release in mice. Male C57BL/6 mice had ICV injection of PBS or famotidine (0.04 or 0.4 mg/kg in 5 μ l volume) 30 min before LPS. LPS was administered IP at 7 mg/kg. Mice were euthanized 2.5 h post-LPS injection and serum and spleen were harvested for analyses. N = 5 for normal group. N = 10 for FM alone. N = 13 or 14 for other groups. * $P < 0.05$, ** $P < 0.01$, *** $P < 0.001$, **** $P < 0.0001$

for a single dose. As LPS elicits significant lethality over a period of several days, we also determined the effect of repeated administration of famotidine on the survival. In C57BL/6 mice subjected to LPS (6 mg/kg, intraperitoneally), treatment with famotidine (4 mg/kg, injected IP, twice daily for 3 days) significantly improved 2-week survival by ~30% compared to mice administered vehicle (Fig. 1E).

Intracerebroventricular administration increases the potency of famotidine.

Human studies have shown that only ~9% of an intravenous dose of famotidine pass through the intact blood brain barrier (Kagevi et al. 1987). Since the inflammatory response is coordinated in part within the CNS/brain (Pavlov et al. 2018), we determined whether central administration of famotidine increased efficacy. Accordingly, famotidine was administered ICV (0.04 or 0.4 mg/kg or vehicle, in 5 μ l volume) 30 min prior to LPS (IP, 7 mg/kg) and pro-inflammatory cytokines assessed after

2.5 h. Famotidine delivered via the ICV route required one tenth of the systemic route to block endotoxin-induced TNF levels in serum by 75% and in the spleen by 84% versus vehicle treated controls (Fig. 2A, C). Likewise, LPS-induced serum and spleen IL-6 were reduced in a famotidine dose-dependent manner (Fig. 2B, D). In confirmation of this effect, tiotidine, a H2R specific antagonist of chemical structure very similar to famotidine (Panula et al. 2015), resulted in identical cytokine suppression when administered ICV (Additional file 1: Fig. S2A–D). In contrast, administration of the first and second generation H2R antagonists cimetidine and ranitidine did not suppress LPS-associated pro-inflammatory cytokine production and did not improve survival (Additional file 1: Fig. S2E–P). Unlike peripheral administration, 6 h after LPS exposure famotidine ICV injection significantly suppressed elevated serum levels of IL-6, but not IL-1 β (Additional file 1: Fig. S3A, B).

Major cellular targets of LPS are not directly inhibited by famotidine.

Mast cells have been hypothesized to drive severe COVID-19 (Malone, et al. 2020; Lam et al. 2021) and LPS activates mast cells to release key pro-inflammatory mediators, including IL-6 (Leal-Berumen et al. 1994). To clarify whether mast cells contribute to famotidine's anti-inflammatory effect, mast cell deficient *Kit^{W-sh}/Kit^{W-sh}* sash mice were employed. This mouse carries a spontaneous *Kit* "sash" mutation, resulting in a universal lack of mast cells (Wolters et al. 2005) and has been used successfully to study mast cell function (Zhang et al. 2019; Weigand et al. 2009). *Kit^{W-sh}/Kit^{W-sh}* sash mice exhibited similar cytokine (serum and splenic TNF, IL-6 and IL-1 β) responses to LPS administration, as compared to wild type (Fig. 3A–F). Administration of famotidine significantly suppressed LPS-induced both TNF and IL-6 release at 2.5 h in the serum and within the spleen in these mice (Fig. 3G–J). Another key target of LPS activation is the macrophage. However, famotidine (0 to 30 μ M) did not significantly inhibit LPS-induced TNF and IL-6 release in murine macrophage-like RAW 264.7 cells in vitro or in pro-inflammatory (thioglycollate-treated) primary mouse macrophages (Fig. 3K–N). Thus, famotidine does not directly antagonize LPS-induced cytokine release by either mast cells or macrophages.

Famotidine activates the inflammatory reflex

To determine whether ICV administration of famotidine induces efferent vagus nerve signaling, we recorded vagus nerve activity in real time following ICV famotidine administration. A micro cuff recording electrode was implanted on the cervical vagus nerve in wildtype mice prior to famotidine administration. ICV administration of famotidine significantly increases vagus nerve electrical activity, in contrast to no change in activity was observed following injection of saline (Fig. 4A, B). When comparing post injection vagus nerve activity, famotidine administration induces significantly more

spikes than saline administration (Fig. 4C). Together, these data suggest that central administration of famotidine has a direct effect on vagus nerve signaling to the periphery.

The vagus nerve consists of both afferent (sensory) and efferent (motor) fibers which mediate anti-inflammatory activity via the inflammatory reflex which is integrated in the brain stem (Chavan et al. 2018). To determine whether famotidine-mediated anti-inflammatory effects depend upon the vagus nerve, the effects of famotidine on LPS toxicity in mice having undergone surgical vagotomy (bilateral sub-diaphragmatic with transgastric pyloric dilation) was assessed. Following vagotomy, famotidine had no effect on LPS-induced levels of TNF or IL-6 at 2.5 h post-LPS injection (Fig. 5 A–D). Stimulating the vagus nerve culminates in acetylcholine release which ultimately mediates inhibits cytokine release by activating α 7nAChR on immune competent cells (Chavan et al. 2018; Bernik et al. 2002). To determine if α 7AChR is required for famotidine-dependent inhibition of cytokines, α 7AChR knockout mice were treated with famotidine during cytokine storm. Inhibition of pro-inflammatory cytokine production by famotidine was greatly attenuated in α 7AChR KO mice (Fig. 6A–D), which also suffered increased mortality (Fig. 6E). Together these observations show that the anti-inflammatory effects of famotidine are dependent upon activation of the vagus nerve inflammatory reflex which requires α 7AChR.

Discussion

The results of the present study provide evidence that in the setting of endotoxin-induced cytokine storm famotidine activates a potent suppression of pro-inflammatory cytokines leading to improved survival. Mechanistically, famotidine inhibits cytokine release via vagus nerve signaling, as evidenced by the observation of increased vagus nerve activity following famotidine administration and loss of anti-inflammatory activity following vagotomy.

(See figure on next page.)

Fig. 3 The mast cell and macrophage are not targets for famotidine. **A–F** Mast cell deficient *Kit^{W-sh}/Kit^{W-sh}* sash mice had similar LPS-induced TNF, IL-6, IL-1 β response as wild type mice. Male wild type (WT) or "sash" mice received LPS injection (IP, 7 mg/kg) and were euthanized 2.5 h post-LPS injection. Serum and spleen TNF, IL-6 and IL-1 β were measured. N = 3. **G–J** Famotidine, administered ICV, reduced LPS-induced TNF and IL-6 release in mast cell deficient *Kit^{W-sh}/Kit^{W-sh}* sash mice at 2.5 h post LPS exposure. Male *Kit^{W-sh}/Kit^{W-sh}* sash mice received famotidine or PBS (0.4 mg/kg, in 5 μ l volume) administered ICV at 30 min prior to LPS injection (IP, 7 mg/kg). Mice were euthanized 2.5 h post-LPS injection and serum TNF and IL-6 were measured. N = 3 for normal wild type, n = 4 for normal "sash", 5 for LPS, 5 or 7 for LPS + famotidine group. *P < 0.001. **P < 0.0001. **K–N** RAW 264.7 cells (K–L) or thioglycollate-elicited mouse primary peritoneal macrophages (M–N) in 96-well culture plates were stimulated with LPS (0.4 ng/ml) in combination with various amounts of famotidine for 16 h. TNF (K,M) and IL-6 (L,N) released in the supernatants were measured. n = 3–6 per treatment. *P < 0.05 vs. LPS alone

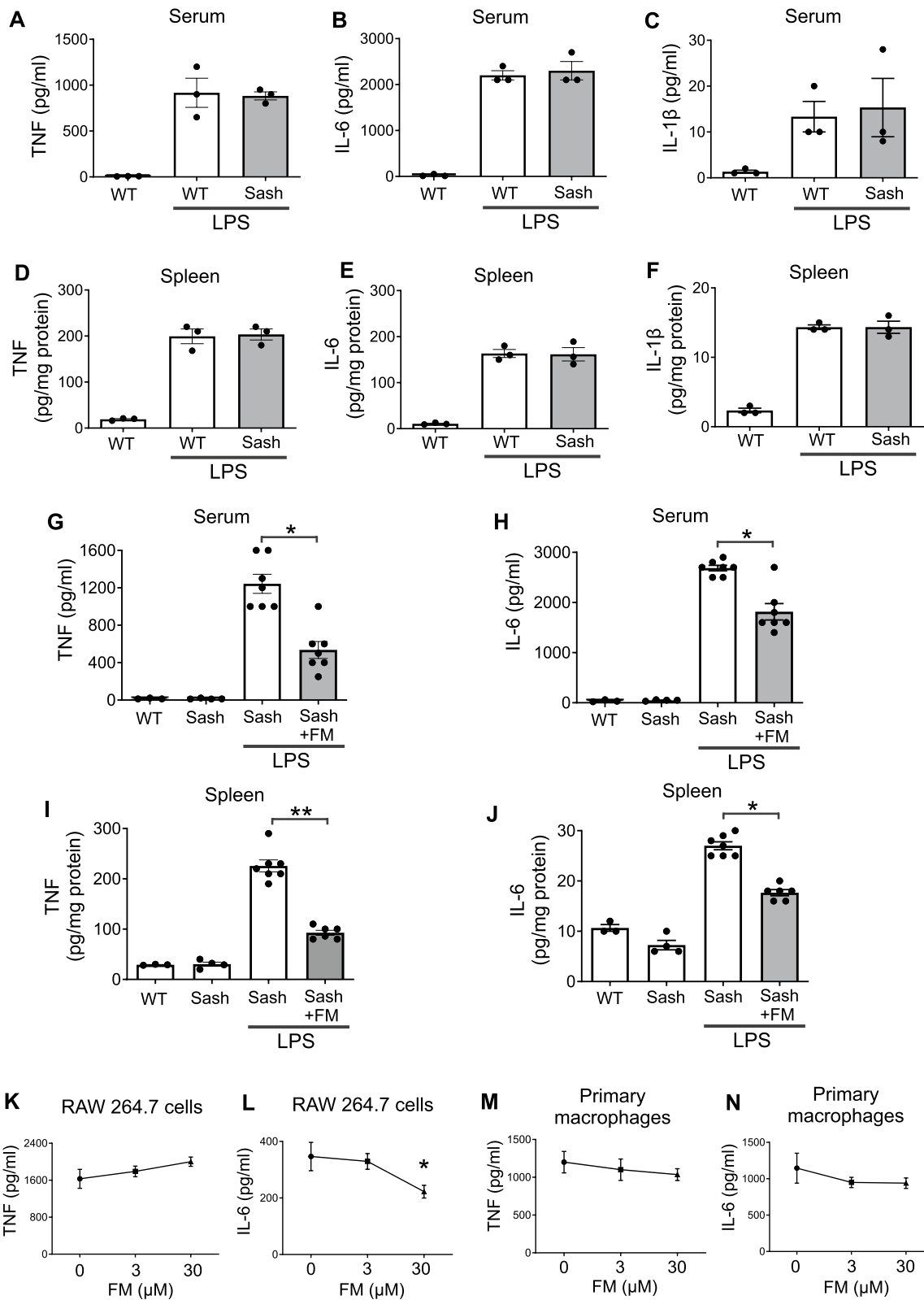
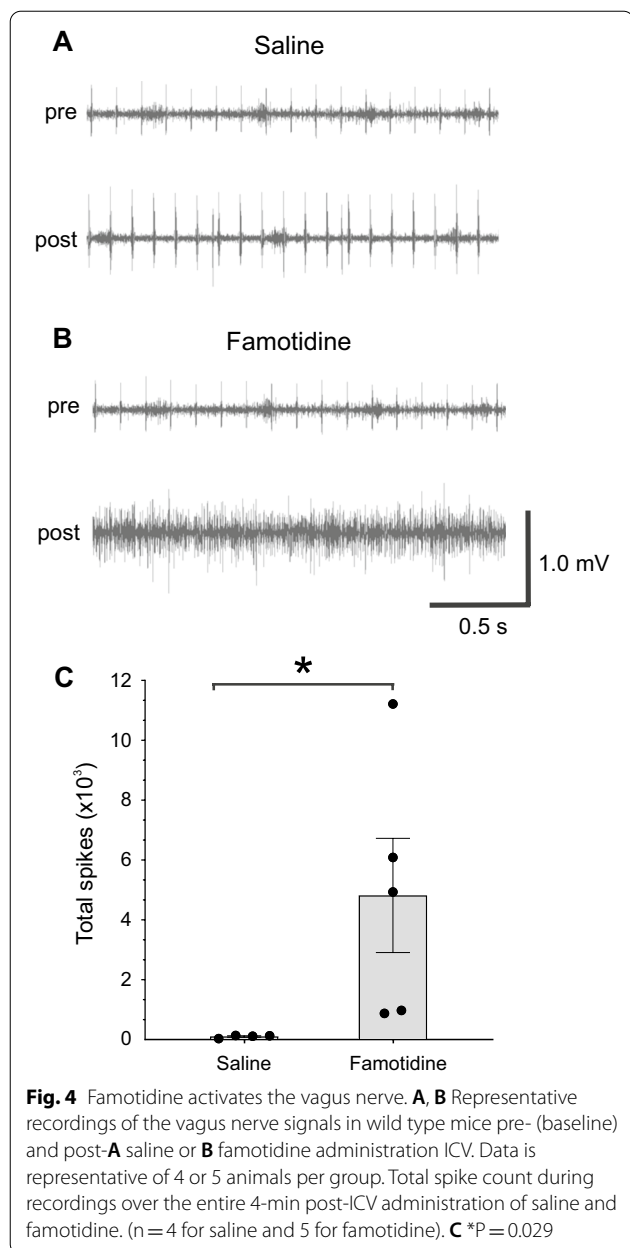


Fig. 3 (See legend on previous page.)

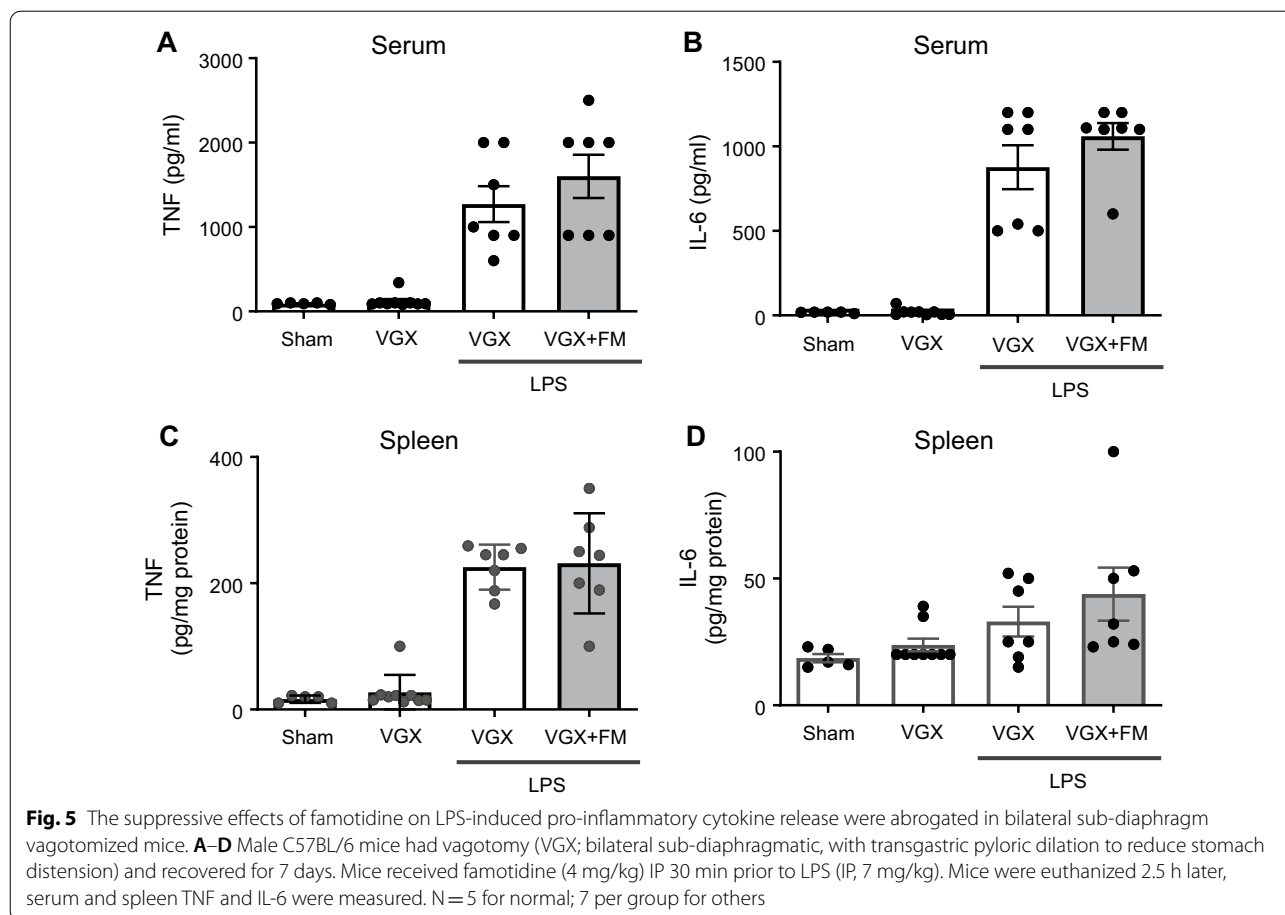


This anti-inflammatory activity depends on the $\alpha 7$ AChR, and based upon the results of previous study, are attributable to the inhibition of $\alpha 7$ AChR positive macrophage pro-inflammatory cytokine release (Wang et al. 2003). A prior study has also identified the existence of anti-inflammatory neural pathways operating via efferent projections from the dorsal motor nucleus (DMN) directly to visceral organs, e.g., the intestines, which

could reasonably explain these observations (Olofsson et al. 2012). In support of this hypothesis, direct administration of famotidine, or the structurally related H2R antagonist tiotidine into the ventricular system in close proximity to the DMN, reduced LPS-induced pro-inflammatory cytokine release at one tenth the amount required when delivered via the intraperitoneal route. Future investigation will need to focus on the effects of famotidine on the DMN as well as its widely ranging interconnections to other locations within the brain to explore this possibility further.

In contrast, both cimetidine and ranitidine, relatively selective lower potency H2R antagonists, were ineffective even when administered ICV, suggesting strongly that the anti-inflammatory activity of famotidine (and tiotidine) occur via an off-target effect. This discrepancy cannot be explained simply by the tissue concentrations of cimetidine or ranitidine being below the IC_{50} of the H2R. Specifically, direct observation has shown that an ~threefold increase above the IC_{50} is required to fully antagonize H2R in vivo (Lin 1991). Although systemic concentrations of cimetidine administered would not likely have reached a threefold higher than IC_{50} concentration (~1.5 μ M (Panula et al. 2015)), the maximum dose administered directly into the small CSF volume of the mouse (~35 μ l (Pardridge 2016)) would exceed the IC_{50} by a factor of ~5000. Similar considerations apply to ranitidine, with an IC_{50} for H2R of ~0.2 μ M.

Two additional activities of H2R antagonists have been reported which could directly affect inflammatory processes. First, famotidine has documented powerful antioxidant effects in vitro, particularly for scavenging nitric oxide (Ahmadi et al. 2011), the hydroxyl radical (Ching et al. 1993), and myeloperoxidase-catalyzed reactions (Zyl et al. 1993) which could serve to directly reduce inflammation. However, this effect cannot explain the current observations as cimetidine and ranitidine also are potent antioxidants, which is explained a critical sulfur atom as a component of the molecular structures (Ching et al. 1994). Additionally, antioxidative effects would not explain the dependency of an intact vagus nerve on the observed anti-inflammatory effects. A second potentially relevant biological activity is the documented weak anti-cholinesterase activity of H2R antagonists (Aono et al. 1986) which could theoretically lead to direct activation of $\alpha 7$ nACh and thereby inhibiting the release of pro-inflammatory mediators. However, similar to the case of antioxidant activity,



the fact that an intact vagus nerve is required for anti-inflammatory activity as well as the observation that both cimetidine and ranitidine possess anticholinesterase activity rule this out as a possible explanation. Further study will be required to evaluate these possibilities.

It should be noted that the current study has specifically addressed the activity of famotidine in the setting of severe inflammation caused by a model of cytokine storm and therefore the relevance of the activation of the inflammatory reflex under conditions of milder inflammatory conditions, e.g., mild to moderate symptomatic COVID-19, is currently unclear. Considering this uncertainty, future clinical study to evaluate famotidine’s potential beneficial effects should focus on documenting modulation of pro-inflammatory cytokines in the setting of severe COVID-19, as the

inflammatory reflex may be of less importance in mildly symptomatic disease.

Finally, the ability of famotidine to activate the inflammatory reflex suggests that famotidine may offer therapeutic benefit in a wide variety of disease processes driven by inflammation. Direct electrical stimulation of the vagus nerve, and thereby activation of the inflammatory reflex, has shown benefit in diverse preclinical models (Chavan et al. 2018) as well as clinical trials, e.g., drug resistant rheumatoid arthritis (Koopman et al. 2016) or inflammatory bowel disease (Bonaz et al. 2016). Famotidine, a well-tolerated oral drug, could offer an additional method of activating the inflammatory reflex to reduce pro-inflammatory cytokine generation and resultant tissue damage generated by diverse disease processes.

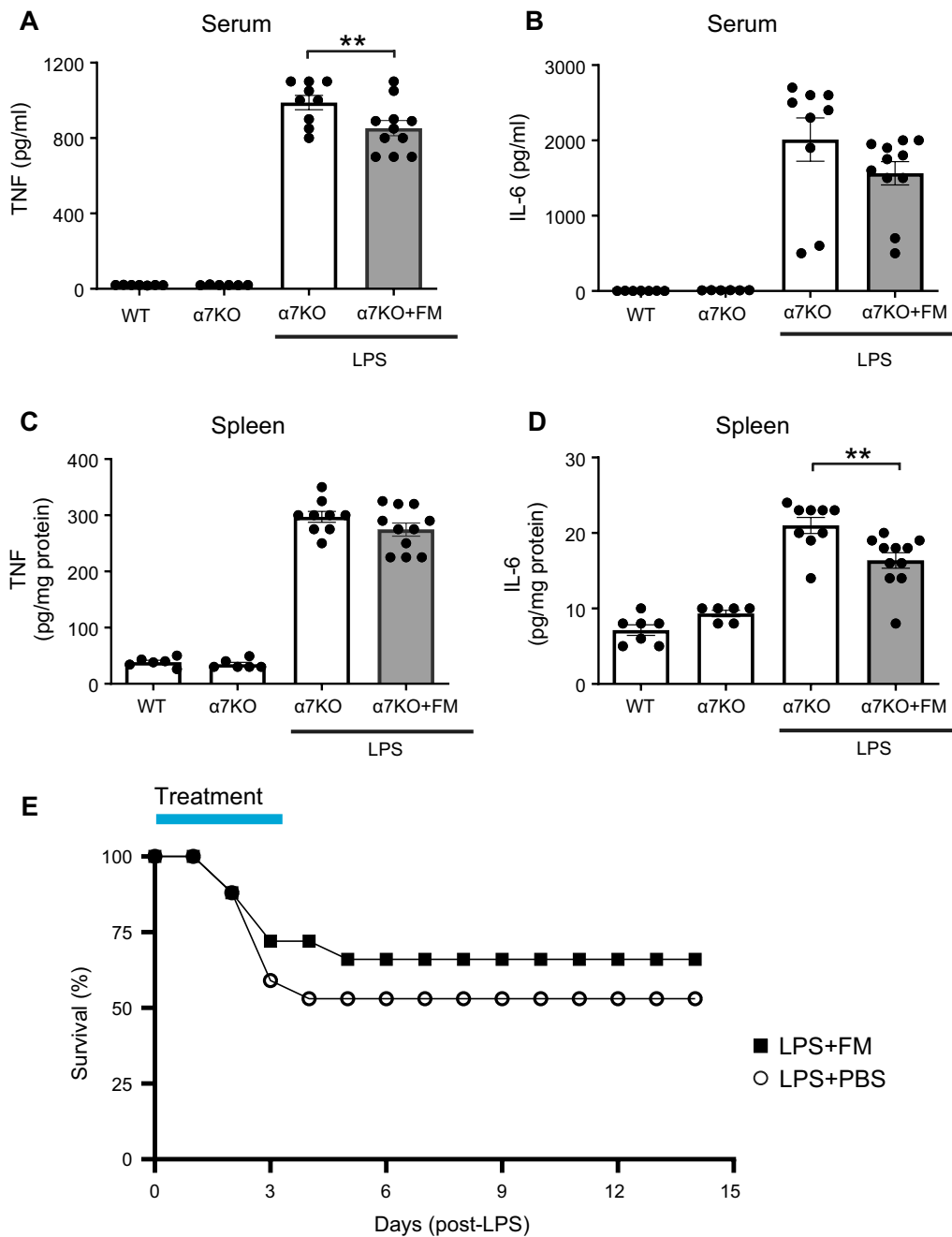


Fig. 6 Suppressive effects of famotidine on LPS-induced TNF and IL-6 release were greatly attenuated and mortality increased in $\alpha 7$ nicotinic acetylcholine receptor knockout mice. **A–D** Male C57BL/6 or $\alpha 7$ nAChR knockout mice ($\alpha 7$ KO; 8–12 weeks of age) received famotidine or PBS (0.4 mg/kg, in 5 μ l volume) administered ICV at 30 min prior to LPS injection (IP, 7 mg/kg). Mice were euthanized 2.5 h post-LPS injection, serum and spleen TNF (**B, C**) and IL-6 (**D, E**) were measured. N = 7 for wild type and 6 for $\alpha 7$ nAChR KO controls, 9–11 per group for others. **E** Male $\alpha 7$ nAChR knockout mice, 8–12 weeks old, were injected with LPS (6 mg/kg, IP). Famotidine (FM) or PBS (4 mg/kg, in 100 μ l volume) were injected intraperitoneally twice a day for 3 days, survival was monitored for 2 weeks. N = 17 for PBS control and 18 for FM mice per group

Abbreviations

FM: Famotidine; CM: Cimetidine; HMGB1: High mobility group box 1; SARS-CoV-2: Severe acute respiratory syndrome coronavirus 2; ICV: Intracerebroventricular; LPS: Lipopolysaccharide; IP: Intraperitoneal; KO: Knockout; H2R: Histamine 2 receptor; VGX: Vagotomy; ELISA: Enzyme-linked immunosorbent assay; PBS: Phosphate buffered saline; TNF: Tumor necrosis factor; IL: Interleukin;

CXCL1: Chemokine (C-X-C motif) ligand 1; $\alpha 7$ nAChR: Alpha 7 nicotinic acetylcholine receptor; WT: Wild type; ANOVA: Analysis of variance.

Supplementary Information

The online version contains supplementary material available at <https://doi.org/10.1186/s10020-022-00483-8>.

Additional file 1: Figure S1. Intraperitoneal administration of famotidine did not significantly alter IL-1 β or CXCL1 levels at 2.5 or 6 h post LPS exposure. **A–D** Male C57BL/6 mice, 8–12 weeks of age, were injected with LPS (7 mg/kg) with or without famotidine (FM, 0.4 or 4 mg/kg, in 100 μ l volume), intraperitoneally 30 min before LPS injection. Mice were euthanized 2.5 h after LPS or FM administration. Serum and spleen IL-1 β and CXCL1 were measured (N = 10 mice per group), as well as serum IL-6 (N = 5 mice per group). **E–H** Mice received an IP injection of famotidine or vehicle (0.04 or 0.4 mg/kg, in 5 μ l volume) 30 min before LPS injection. LPS was administered IP at 7 mg/kg. Mice were euthanized 6 h post-LPS injection. N = 5 for normal group. N = 13–14 for others. **Figure S2.** Effects of other histamine 2 receptor antagonists. **A–D** Male C57BL/6 mice had ICV injection of PBS or tiotidine (0.04 or 0.4 mg/kg in 5 μ l volume) 30 min before LPS. LPS was administered IP at 7 mg/kg. Mice were euthanized 2.5 h post-LPS injection and levels of serum and spleen TNF and IL-6 were measured. N = 5 for normal group. N = 4 for tiotidine 4 mg/kg group and N = 8 for other groups. *P < 0.02, ***P < 0.0001. **E–K** Male C57BL/6 mice, 8–12 weeks of age, received cimetidine or PBS (vehicle) via ICV injection 30 min prior to LPS (IP, 7 mg/kg). Mice were euthanized 2.5 h later and serum and spleen cytokines were measured. N = 3–6 for normal group, N = 9 for other groups. **L–O** Male C57BL/6 mice had ICV injection of PBS, ranitidine (0.4 mg/kg in 5 μ l volume) 30 min before LPS. LPS was administered IP at 7 mg/kg. Mice were euthanized 2.5 h post-LPS injection and levels of serum and spleen TNF and IL-6 were measured. N = 5 for normal group, N = 8 for LPS + PBS and N = 10 for LPS + ranitidine group. *P \leq 0.05. **P** Male C57BL/6 mice, 8–12 weeks old, were injected with LPS (6 mg/kg, IP). CM or PBS (4 mg/kg, in 100 μ l volume) were injected intraperitoneally twice a day for 3 days, survival was monitored for 2 weeks. N = 10 mice (LPS + cimetidine) or 30 (LPS + PBS) per group. **Figure S3.** Famotidine (ICV administration) attenuates lipopolysaccharide (LPS)-induced IL-6 release in mice at 6 h post-LPS administration. A, B. Male C57BL/6 mice, 8–12 weeks of age, were injected with LPS (7 mg/kg) with or without famotidine (FM, 0.04 or 0.4 mg/kg) administered ICV at 30 min before LPS injection. Mice were euthanized 2.5 h after LPS administration. Serum IL-6 and IL-1 β were measured. N = 5 mice per group for normal, 4 or 8 for LPS alone, 10–15 for other groups. *P = 0.008.

Acknowledgements

Not applicable.

Author contributions

HY, MB, SSC, and KJT conceived project, designed experiments and analyzed data. SJG, DAT, HY, HAS, TT, and AT performed experiments. HY, MB, HAS, EHC, VAP, UA, SSC, and KJT wrote the manuscript. All authors discussed the results and commented on the manuscript. All authors read and approved the final manuscript.

Funding

This work was supported in part by grant NIH, NIGMS 1R35GM118182, to KJT R01GM132672 to SSC.

Data availability

The datasets analyzed during the current study are available from the corresponding author on reasonable request.

Declarations

Ethics approval and consent to participate

Not applicable.

Consent for publication

Not applicable.

Competing interests

HY, SSC and KJT are co-inventors of a patent application (Role of the central nervous nerve system and vagus nerve signaling in famotidine-mediated anti-inflammatory effects). All other authors declare no competing interests.

Author details

¹Institute for Bioelectronic Medicine, The Feinstein Institutes for Medical Research, 350 Community Drive, Manhasset, NY 11030, USA. ²Elmazzi Graduate School of Molecular Medicine, Feinstein Institutes for Medical Research, Northwell Health, Manhasset, NY, USA. ³Donald and Barbara Zucker School of Medicine at Hofstra/Northwell, Hempstead, NY, USA. ⁴Department of Women's and Children's Health, Karolinska Institute, Karolinska University Hospital, 17176 Stockholm, Sweden.

Received: 5 April 2022 Accepted: 25 April 2022

Published online: 16 May 2022

References

- Aguila EJT, Cua IHY. Repurposed GI Drugs in the Treatment of COVID-19. *Dig Dis Sci.* 2020;65:2452–3.
- Ahmadi A, et al. Hepatoprotective, antinociceptive and antioxidant activities of cimetidine, ranitidine and famotidine as histamine H2 receptor antagonists. *Fundam Clin Pharmacol.* 2011;25:72–9.
- Aono M, Moriga M, Mizuta K, Narusawa H. Cholinergic effects of histamine-H2 receptor antagonists partly through inhibition of acetylcholinesterase. *Gastroenterol Jpn.* 1986;21:213–9.
- Bernik TR, et al. Pharmacological stimulation of the cholinergic antiinflammatory pathway. *J Exp Med.* 2002;195:781–8.
- Bonaz B, et al. Chronic vagus nerve stimulation in Crohn's disease: a 6-month follow-up pilot study. *Neurogastroenterol Motil.* 2016;28:948–53.
- Brennan CM, et al. Oral famotidine versus placebo in non-hospitalised patients with COVID-19: a randomised, double-blind, data-intensive, phase 2 clinical trial. *Gut.* 2022;79:871.
- Chavan SS, Ma P, Chiu IM. Neuro-immune interactions in inflammation and host defense: Implications for transplantation. *Am J Transplant.* 2018;18:556–63.
- Ching TL, Haenen GR, Bast A. Cimetidine and other H2 receptor antagonists as powerful hydroxyl radical scavengers. *Chem Biol Interact.* 1993;86:119–27.
- Ching TL, de Jong J, Bast A. Structural characteristics of histamine H2 receptor antagonists that scavenge hypochlorous acid. *Eur J Pharmacol.* 1994;268:89–93.
- DeVos SL, Miller TM. Direct intraventricular delivery of drugs to the rodent central nervous system. *J vis Exp.* 2013;34:e50326.
- Dezfuli G, et al. Subdiaphragmatic vagotomy with pyloroplasty ameliorates the obesity caused by genetic deletion of the melanocortin 4 receptor in the mouse. *Front Neurosci.* 2018;12:104.
- Ennis M, Tiligada K. Histamine receptors and COVID-19. *Inflamm Res.* 2020;89:1–9.
- Freedberg DE, et al. Famotidine Use Is Associated With Improved Clinical Outcomes in Hospitalized COVID-19 Patients: A Propensity Score Matched Retrospective Cohort Study. *Gastroenterology.* 2020;159:1129–1131. e1123.
- Gauthier AG, et al. From nicotine to the cholinergic anti-inflammatory reflex - Can nicotine alleviate the dysregulated inflammation in COVID-19? *J Immunotoxicol.* 2021;18:23–9.
- Haas HL, Sergeeva OA, Selbach O. Histamine in the nervous system. *Physiol Rev.* 2008;88:1183–241.
- Jafarzadeh A, Chauhan P, Saha B, Jafarzadeh S, Nemati M. Contribution of monocytes and macrophages to the local tissue inflammation and cytokine storm in COVID-19: Lessons from SARS and MERS, and potential therapeutic interventions. *Life Sci.* 2020;257: 118102.
- Janowitz T, et al. Famotidine use and quantitative symptom tracking for COVID-19 in non-hospitalised patients: a case series. *Gut.* 2020;69:1592–7.
- Kagevi I, Thorhallsson E, Wahlby L. CSF concentrations of famotidine. *Br J Clin Pharmacol.* 1987;24:849–50.
- Koopman FA, et al. Vagus nerve stimulation inhibits cytokine production and attenuates disease severity in rheumatoid arthritis. *Proc Natl Acad Sci U S A.* 2016;113:8284–9.

- Lam HY, Tergaonkar V, Kumar AP, Ahn KS. Mast cells: Therapeutic targets for COVID-19 and beyond. *IUBMB Life*. 2021;89:45.
- Lapenna D, et al. H2-receptor antagonists are scavengers of oxygen radicals. *Eur J Clin Invest*. 1994;24:476–81.
- Leal-Berumen I, Conlon P, Marshall JS. IL-6 production by rat peritoneal mast cells is not necessarily preceded by histamine release and can be induced by bacterial lipopolysaccharide. *J Immunol*. 1994;152:5468–76.
- Lin JH. Pharmacokinetic and pharmacodynamic properties of histamine H2-receptor antagonists. Relationship between intrinsic potency and effective plasma concentrations. *Clin Pharmacokinet*. 1991;20:218–36.
- Loffredo M, et al. (2020) The Effect of Famotidine on SARS-CoV-2 Proteases and Virus Replication. *bioRxiv*: 2020.2007.2015.203059.
- Malone RW, et al. (2020) COVID-19: Famotidine, Histamine, Mast Cells, and Mechanisms. *Research square*.
- Mehta P, et al. COVID-19: consider cytokine storm syndromes and immunosuppression. *Lancet*. 2020;395:1033–4.
- Moore JB, June CH. Cytokine release syndrome in severe COVID-19. *Science*. 2020;368:473–4.
- Mukherjee R, et al. Famotidine inhibits toll-like receptor 3-mediated inflammatory signaling in SARS-CoV-2 infection. *J Biol Chem*. 2021;297: 100925.
- Nair AB, Jacob S. A simple practice guide for dose conversion between animals and human. *J Basic Clin Pharm*. 2016;7:27–31.
- Olofsson PS, Rosas-Ballina M, Levine YA, Tracey KJ. Rethinking inflammation: neural circuits in the regulation of immunity. *Immunol Rev*. 2012;248:188–204.
- Panula P, et al. International Union of Basic and Clinical Pharmacology. XCVIII Histamine Receptors *Pharmacol Rev*. 2015;67:601–55.
- Pardridge WM. CSF, blood-brain barrier, and brain drug delivery. *Expert Opin Drug Deliv*. 2016;13:963–75.
- Pavlov VA, Chavan SS, Tracey KJ. Molecular and Functional Neuroscience in Immunity. *Annu Rev Immunol*. 2018;36:783–812.
- Ramos-Benitez MJ, et al. Fh15 Blocks the Lipopolysaccharide-Induced Cytokine Storm While Modulating Peritoneal Macrophage Migration and CD38 Expression within Spleen Macrophages in a Mouse Model of Septic Shock. *Sphere*. 2018;3:23789.
- Seemann S, Zohles F, Lupp A. Comprehensive comparison of three different animal models for systemic inflammation. *J Biomed Sci*. 2017;24:60.
- Sharun K, Tiwari R, Dhama J, Dhama K. Dexamethasone to combat cytokine storm in COVID-19: Clinical trials and preliminary evidence. *Int J Surg*. 2020;82:179–81.
- Smuda C, Wechsler JB, Bryce PJ. TLR-induced activation of neutrophils promotes histamine production via a PI3 kinase dependent mechanism. *Immunol Lett*. 2011;141:102–8.
- Steinberg BE, et al. Cytokine-specific Neurograms in the Sensory Vagus Nerve. *Bioelectron Med*. 2016;3:7–17.
- Theoharides TC, Conti P. Dexamethasone for COVID-19? Not so fast. *J Biol Regul Homeost Agents*. 2020;34:1241–3.
- van Zyl JM, Kriegler A, van der Walt BJ. Anti-oxidant properties of H2-receptor antagonists. Effects on myeloperoxidase-catalysed reactions and hydroxyl radical generation in a ferrous-hydrogen peroxide system. *Biochem Pharmacol*. 1993;45:2389–97.
- Wang H, et al. Nicotinic acetylcholine receptor alpha7 subunit is an essential regulator of inflammation. *Nature*. 2003;421:384–8.
- Wang J, Jiang M, Chen X, Montaner LJ. Cytokine storm and leukocyte changes in mild versus severe SARS-CoV-2 infection: Review of 3939 COVID-19 patients in China and emerging pathogenesis and therapy concepts. *J Leukoc Biol*. 2020;108:17–41.
- Weigand LA, Myers AC, Meeker S, Udem BJ. Mast cell-cholinergic nerve interaction in mouse airways. *J Physiol*. 2009;587:3355–62.
- Wolters PJ, et al. Tissue-selective mast cell reconstitution and differential lung gene expression in mast cell-deficient Kit(W-sh)/Kit(W-sh) sash mice. *Clin Exp Allergy*. 2005;35:82–8.
- Wu C, et al. Analysis of therapeutic targets for SARS-CoV-2 and discovery of potential drugs by computational methods. *Acta Pharmaceutica Sinica B*. 2020;10:766–88.
- Yang H, et al. MD-2 is required for disulfide HMGB1-dependent TLR4 signaling. *J Exp Med*. 2015;212:5–14.
- Zanos TP, et al. Identification of cytokine-specific sensory neural signals by decoding murine vagus nerve activity. *Proc Natl Acad Sci U S A*. 2018;115:E4843–52.
- Zhang T, et al. A Mast Cell-Specific Receptor Is Critical for Granuloma Induced by Intrathecal Morphine Infusion. *J Immunol*. 2019;203:1701–14.

Publisher's Note

Springer Nature remains neutral with regard to jurisdictional claims in published maps and institutional affiliations.

Ready to submit your research? Choose BMC and benefit from:

- fast, convenient online submission
- thorough peer review by experienced researchers in your field
- rapid publication on acceptance
- support for research data, including large and complex data types
- gold Open Access which fosters wider collaboration and increased citations
- maximum visibility for your research: over 100M website views per year

At BMC, research is always in progress.

Learn more biomedcentral.com/submissions

